Annals of Phytomedicine 14(1): 569-579, 2025

DOI: http://dx.doi.org/10.54085/ap.2025.14.1.54

Annals of Phytomedicine: An International Journal
http://www.ukaazpublications.com/publications/index.php

Print ISSN : 2278-9839 Online ISSN : 2393-9885

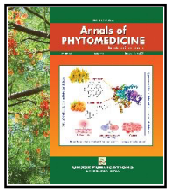

Original Article : Open Access

Pharmacological evaluation and cytotoxic assessment of *Ceriops tagal* (Perr.) C.B. Rob. metabolites with comprehensive analytical and ADMET insights against Glioblastoma multiforme

Monica Murugesan*, Sankar Natesan and Priyatharsini Rajendran*◆**

* *Department of Zoology and Research Centre, Lady Doak College, Madurai Kamaraj University, Thallakulam, Madurai-625 002, Tamil Nadu, India*

** *Department of Genetic Engineering, School of Biotechnology, Madurai Kamaraj University, Madurai-625 021, Tamil Nadu, India*

Article Info

Article history
Received 2 January 2024
Revised 16 February 2025
Accepted 17 February 2025
Published Online 30 June 2025

Keywords
Ceriops tagal (Perr.) C.B. Rob.
Secondary metabolites
Anti-glioblastoma
Cytotoxicity
Cell cycle arrest
FUCCI biosensor
HPTLC
GC-MS

Abstract

Mangrove plants, particularly halo-tolerant species such as *Ceriops tagal*, (Perr.) C.B. Rob. (CT) serve as valuable sources of bioactive compounds, with therapeutic potential including anticancer properties. These compounds exhibit diverse biological activities and are employed in treating diseases and degenerative conditions. This study investigates the secondary metabolites present in the methanol leaf extract of *C. tagal*, focusing on their pharmacokinetic properties, anti-glioblastoma activity, and cell cycle arrest mechanisms. The detection of secondary metabolites, such as flavonoids, phenols, saponins, and alkaloids was achieved through chromatographic methods like high-performance thin layer chromatography (HPTLC) and gas-chromatography-mass spectrometry (GC-MS). Identified compounds were classified using the ClassyFire software tool to ascertain compound diversity. Cytotoxicity assays were conducted to determine IC_{50} values, while cell cycle analysis utilized the FUCCI biosensor in a flow cytometer to explore the effects on Glioblastoma multiforme (GBM) cells. HPTLC fingerprinting analysis revealed quenching at 366 nm confirming the presence of phenols, flavonoids, saponins and alkaloids. The CT extract exhibited strong cytotoxic effect with an IC_{50} of 1.47 µg/ml, which is significantly more potent than the standard GBM chemotherapeutic drug, temozolomide. The CT extract induced G1/S phase arrest in GBM cells, a key mechanism that can prevent cell proliferation and contribute to its anticancer efficacy. *In silico* ADMET (absorption, distribution, metabolism, excretion and toxicity) analyses confirmed favourable pharmacokinetic properties for the identified metabolites, with 54 out of 93 compounds selected based on drug-likeness and nine compounds were predicted to be non-toxic. These promising findings indicate that *C. tagal* metabolites hold significant potential as therapeutic agent against GBM, but further investigation is needed to fully elucidate their mechanism of action and therapeutic applicability.

1. Introduction

Halophytes are salt-resistant plants that offer various economic advantages, including ecological restoration and medicinal applications. It includes mangroves and their associates, which thrive in tropical and subtropical coastal regions, are vital not only for ecosystem stability during natural disasters but also for their bioactive compounds with therapeutic potential (Eswaraiah *et al.,* 2020; Kiran Kumar and Pola, 2022). Natural products account for approximately 60% of clinically approved drugs, with marine flora emerging as a significant resource for anticancer drug development (Boopathy *et al.*, 2011; Cragg and Newman, 2005). Marine flora, particularly mangroves have gained attention for their diverse secondary metabolites, which exhibit pharmacological properties such as antioxidant and anticancer activities. These metabolites often influence key cellular processes, including cell cycle regulation, protein expression in molecular signaling pathways. Additionally, they have the potential to cross blood-brain barrier (BBB), underscoring their potential as novel cancer therapeutics (Makkar *et al.*, 2020; Tundis *et al.*, 2014).

Polyphenols, a predominant class of bioactive compounds in plants plays significant role in neutralizing reactive oxygen species (ROS) and mitigating oxidative stress-induced damage both of which are implicated in cancer development (Costa *et al.*, 2021; Williams *et al.*, 2004; Verma *et al.*, 2022). Furthermore, plant-deriveds alkaloids for instance, vinca alkaloids effectively target molecular pathways to inhibit tumor progression making them crucial in chemotherapy regimens (Bakrim *et al.*, 2022; Cragg and Newman, 2005; Pandrangi *et al.*, 2022). The synergistic potential of plant-based compounds provides a promising strategy for cancer treatment, as individual plants often produce a complex mixture of metabolites with unique structural diversity and biological activities (Kumar *et al.,* 2021). Despite the abundance of these metabolites, only a fraction has been explored for their pharmacological significance (Pandey *et al.,* 2013).

The true mangrove species, *C. tagal* of Rhizophoraceae family, has shown therapeutic value in traditional medicine for treating malaria and diabetes, particularly in China (Ni *et al.*, 2018). Beyond its

Corresponding author: Dr. Priyatharsini Rajendran
Associate Professor and Head, Department of Zoology and Research Centre, Lady Doak College, Madurai-625 002, Tamil Nadu, India
E-mail: priyatharsinirajendran@ldc.edu.in
Tel.: +91-9486071644

traditional uses, CT demonstrates a wide spectrum of pharmacological activities, including anticancer, antitumor, antibacterial, antifungal, antidiabetic, and antioxidant properties (Arivuselvan *et al.*, 2011; Chacha, 2012; Tiwari *et al.*, 2008)). Phytochemical analyses of CT has identified bioactive compounds such as polyphenols, alkaloids, saponins, terpenoids, glycosides, and sterols (Manohar *et al.*, 2023; Zhang *et al.*, 2005).

GBM, an aggressive and heterogeneous brain tumor, affects approximateasly 3.5 cases per 100,000 people globally, with a mortality rate of 2.8 per 100,000 individuals. It accounts for 48-49% of all malignant primary brain tumors with higher incidence in men and regions such as North America and Europe (Global Cancer Observatory Report, 2022). Existing treatment such as surgical resection, radiation, and chemotherapy, extend the median survival rate to only 6-15 months (Fisher and Adamson, 2021; Jain, 2018; Krex *et al.,* 2007). The limitations of current GBM treatments, including poor prognosis, restricted blood-brain barrier (BBB) permeability, high recurrence rates, invasiveness, and the severe side effects of radiation and chemotherapy, highlight the need for alternative therapies. Plant-derived polyphenols, known for their safety compared to synthetic drugs, offer a promising approach to overcoming these challenges and improving treatment outcomes (Sun *et al.,* 2009).

The fluorescent ubiquitination-based cell cycle indicator (FUCCI) is an innovative biosensor used in live-cell imaging to monitor cell cycle progression in real-time. This system employs fluorescent proteins linked to cell cycle-specific degron domains, enabling distinct color changes that correspond to different phases of the cell cycle (Sakaue-Sawano *et al*., 2008). During the G1 phase, cells emit red fluorescence due to the presence of mKO_2-tagged Cdt1. As cells transition into the S, G2, and M phases, green fluorescence appears due to the accumulation of mAG-tagged geminin. A combination of both red and green fluorescence results in a yellow hue, indicating the transition between the G1 and S phases. FUCCI has been extensively applied in cell cycle research, oncology, and developmental biology, as it enables real-time visualization of proliferative activity.

Therefore, this study utilized advanced chromatographic techniques to identify and validate bioactive compounds in methanol extracts of CT leaves. For the first time, the *in vitro* anticancer potential against GBM cells using CT extract was assessed. Computational tools were utilized to assess the pharmacokinetic characteristics of the compounds identified, while the effects on cell cycle arrest were analyzed using the FUCCI biosensor system, a state-of-the-art method for monitoring cell cycle dynamics.

2. Materials and Methods

2.1 Plant authentication

The plant was authenticated by Dr.Ramanathan, Associate Professor at the CAS in Marine Biology, Parangipettai, Tamil Nadu, India. The Voucher Specimen Number (LDCBTH1802) was deposited in the repository (Murugesan *et al.,* 2020).

2.2 Plant extraction

C. tagal with ethnomedicinal properties was collected from Parangipettai, Tamil Nadu, India (Coordinates: 11°29' 32.5" N and 79°46' 01.9" E). Leaves were shade-dried, finely powdered, and extracted using 250 ml of HPLC-grade methanol at 40°C for 3 h and re-extracted using the same solvent. Extraction was performed in triplicate, and the combined extracts were concentrated using a rotary evaporator (Buchi, Switzerland) and freeze-dried (Christ Alpha 1-2 LD Plus) for storage at 4°C (Abideen *et al.,* 2015). The lyophilized CT extract and the reference drug, temozolomide (TMZ), were dissolved in DMSO to prepare 1 mg/ml stock solutions for cytotoxicity assay. Further dilutions for assays were made in the respective media.

2.3 HPTLC fingerprinting of phytochemicals

High-performance thin-layer chromatography was utilized to detect phenols, flavonoids, alkaloids, and saponins. Methanolic CT extract (1 mg/ml) was applied as 8 mm-wide bands on silica gel plates (Silica Gel 60 F254, Merck) using a Camag Linomat V applicator. Plates were developed with compound-specific mobile phase solvents in a twin-trough chamber pre-saturated for 20 min as listed below. The developed plates were scanned at λ_{max} 254 nm, 366 nm, and 540 nm using CAMAG Scanner 4 and analyzed using Vision CATS software (v.3.1) (Kandler *et al*., 2009).

i. **Phenols:** Cyclohexane: Ethyl acetate: Formic acid (4:6:1)

ii. **Flavonoids:** Ethyl acetate: Formic acid: Acetic acid: Water (10:0.5:0.5:0.5)

iii. **Saponins:** Chloroform: Acetic acid: Methanol: Water (6.4:3.2:1.2:0.8)

iv. **Alkaloids:** Ethyl acetate: Methanol: Water (10:1:1).

2.4 GC-MS profiling of secondary metabolites

Gas chromatographic-mass spectrometry analysis was performed for crude methanolic CT extract using an 7000 D GC-MS system (Agilent Technologies). Separation was carried out using a TR-5MS column (30 m × 0.25 mm × 0.25 µm). Helium served as the carrier gas maintaining a flow rate of 1.0 ml/min. The temperature gradient was programmed from 40°C to 250°C gradually at a temperature of 5°C/min. Data were analyzed using mass hunter software (v.3.6). Chemical structures were retrieved and validated using Swiss ADME (Eswaraiah *et al*., 2020).

2.5 Classification of secondary metabolites

The canonical SMILES obtained from Swiss ADME were then processed using the Classy Fire tool, which classified the identified compounds into categories alkaloids, flavonoids, phenols, and other secondary metabolite classes based on hierarchical chemical taxonomy.

2.6 Cell culture

The human glioblastoma cell line LN229, which contains TP53 mutations and homozygous deletions of p16 and p14ARF, was cultured in dulbecco's modified eagle medium (DMEM) containing 10% FBS, 1% penicillin-streptomycin, and 1X trypsin-EDTA. The

cells were incubated at 37°C in a humidified environment with 5% CO_2 until they reached 70-80% confluence (Doan *et al.*, 2020).

2.7 Cytotoxicity assay

LN229 GBM cells were plated in 6-well plates at a density of 1×10 µ cells per well and exposed to CT and TMZ at concentrations ranging from 0.5 to 15 µg/ml (0.5, 1, 5, 10, and 15 µg/ml) for 48 h. Cell viability was assessed using the trypan blue exclusion assay, and cell counts were determined with a Countess II FL hemocytometer (Thermo Fisher Scientific). IC_{50} values were estimated from dose-response curves generated using GraphPad Prism (v.8.0).

2.8 FUCCI-based cell cycle analysis

Cell cycle arrest in LN229 cells treated with IC_{50} CT was analyzed using the FUCCI BacMam 2.0 cell cycle sensor, following the manufacturer's guidelines. The fluorescent images were acquired with an EVOS microscope and analyzed using flow cytometry (Sysmex Cube 8). The data were subsequently processed and analysed with FlowJo software (v.10.0) (Doan *et al*., 2020).

2.9 ADMET profiling

The ADMET and drug-likeness properties were evaluated using Swiss ADME and pkCSM tools. The pharmacokinetic parameters included gastrointestinal (GI) absorption, blood-brain barrier (BBB) permeability, p-gp substrate/inhibitor classification, and predicted toxicological endpoints such as AMES mutagenicity and hepatotoxicity. Lipinski's rule of five was applied to evaluate the drug-likeness of the compounds (Daina *et al*., 2017).

2.10 Statistical analysis

The results were presented as the mean ± standard error (SE) based on biological and technical replicates (n = 4). Statistical analysis was conducted using one-way ANOVA, followed by Dunnett's post-hoc test in GraphPad Prism (v.8.0.2). A *p*-value of less than 0.05 was regarded as statistically significant.

3. Results

3.1 Polyphenol fingerprinting of CT validated using HPTLC analysis

The crude methanol CT extract at a concentration of 1 mg/ml was analyzed for the presence of polyphenols, including flavonoids, phenols, saponins, and alkaloids. The fingerprinting analysis revealed distinct bands at UV 254 nm and 366 nm, confirming the presence of polyphenols, alkaloids, and saponins. A compound-specific solvent system was used, with the chromatogram showing quenching at UV 366 nm and distinct color bands: violet bands for phenols, blue bands for flavonoids, blue-violet bands for saponins, and blue and yellow bands for alkaloids. The densitogram of the fingerprinting analysis illustrated 4 peaks for phenols and 7 peaks each for flavonoids, saponins, and alkaloids, validating the presence of polyphenols (Figure 1). The retention factors (Rf max) were as follows: phenols (0.032 to 0.648), flavonoids (0.029 to 0.974), saponins (0.035 to 0.995), and alkaloids (0.037 to 0.967).

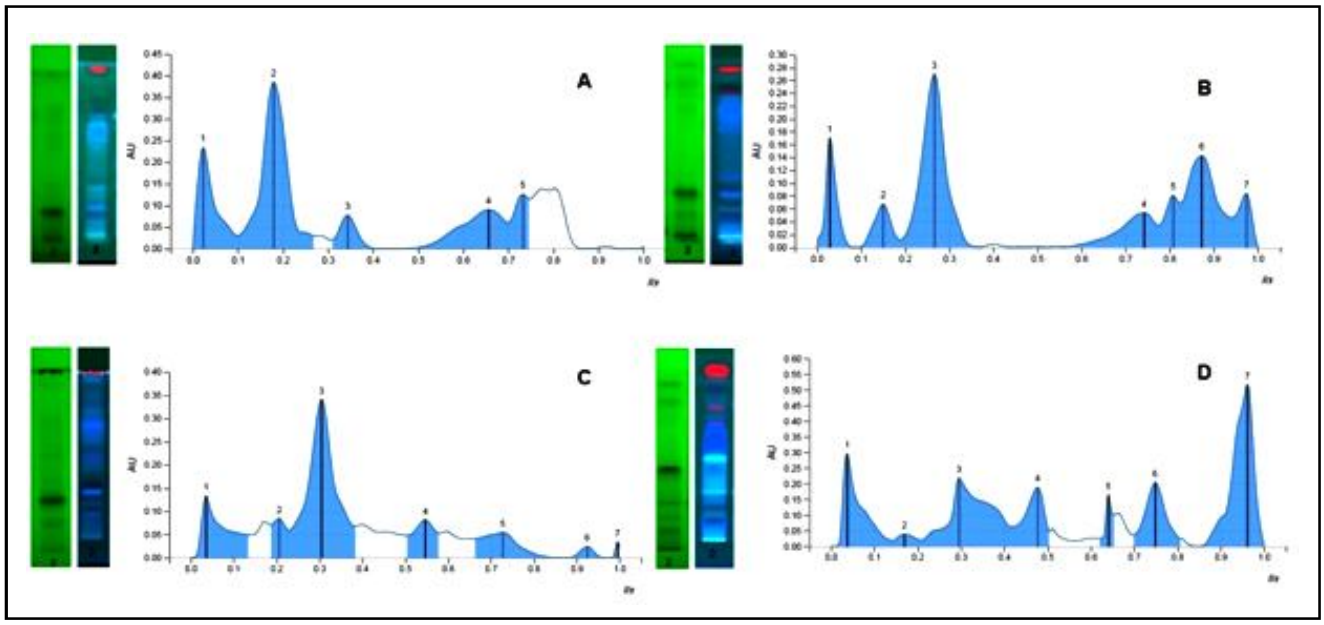

Figure 1: Fingerprinting of secondary metabolites present in CT using HPTLC analysis.

The analysis of the fingerprinting validated the existence of (A) phenols, (B) flavonoids, (C) saponins, and (D) alkaloids accompanied by the respective densitogram with the plate at UV 254 nm and 366 nm for the crude methanol leaf extract of CT.

3.2 CT possesses a diverse class of secondary metabolites

The GC-MS analysis of the crude methanol leaf extract of CT revealed a total of 93 peaks (Figure 2), corresponding to secondary metabolites identified by their retention times (Table 1). Among these, 28 peaks were categorized as major peaks, while 66 were minor peaks. The mass hunter software identified compounds within the CT extract, with notable peaks and retention times as follows:

- Ethanamine, 2-(methylthio)- (RT-2.2677)
- 2(5H)-Furanone (RT-2.6658)
- 1-Butanamine, N-nitro- (RT-2.9027)

- Oxalic acid, cyclobutyl hexyl ester (RT-3.2555)
- 2, 4-Dihydroxy-2, 5-dimethyl-3 (2H)-furan-3-one (RT-3.6628)
- 2-Methyl [1,3,4] oxadiazole (RT-4.0093)

Compounds with potential anticancer effects included 2(5H)-furanone (Wu *et al.*, 2018), 1,2,4-triazole (Kumari *et al.*, 2021), quinoline (Rajesh, 2020), and 12,15-octadecatrienoic acid (Ranjith Kumar *et al.*, 2021; Narmada Devi *et al.*, 2024). The antioxidant properties are displayed by octadecanoic acid (Dasarapu Santhosha and Ramesh Alluri , 2022). These metabolites were categorized into phenols, alkaloids, amines, amino acids, and organoelements such as organofluorine and organosilicon. Among the 93 metabolites, organic compounds had the highest count, followed by organoelements, alkaloids, polyphenols, fatty acids, and amino acids.

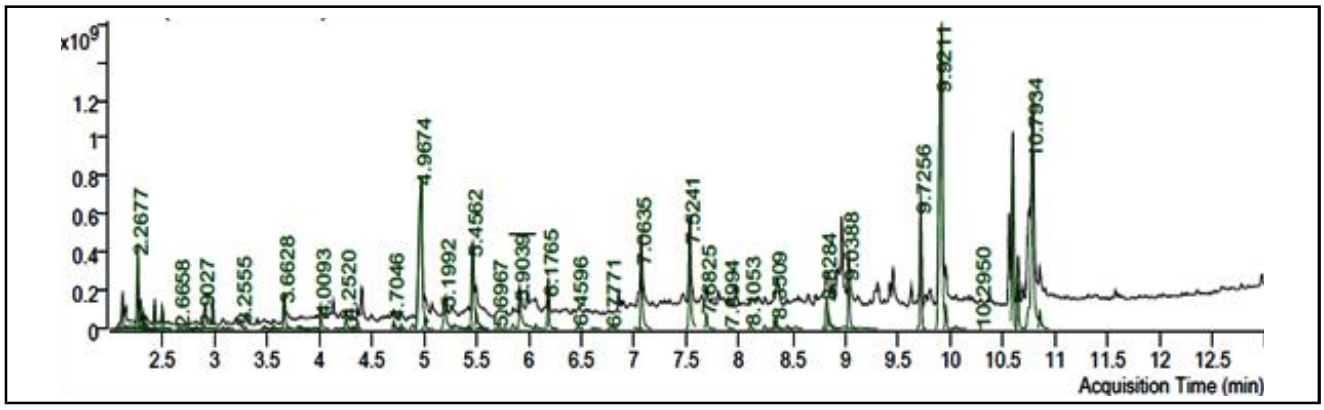

Figure 2: **GC-MS analysis of crude methanol CT extract. Chromatogram of crude CT extract showed the presence of diverse secondary metabolites with retention time (RT).**

Table 1: **GC-MS analysis of the crude CT extract. The analysis using GC-MS of the crude methanolic leaf extract unveiled the identification of 93 metabolites using mass hunter software (Ver.3.6).The compounds each having a specific retention time were categorized based on their functional groups**

S.No.	Retention time (RT)	Chemical name	Chemical formula	Mol. wt. (g/mol)	Classification
1.	2.0742	Methylamine, N,N-dimethyl-	C_3H_9N	59.11	Amines
2.	2.1231	Trifluoroguanidine	$CH_2F_3N_3$	113.04	Alkaloids
3.	2.221	Cyclotrisiloxane, hexamethyl-	$C_6H_{18}O_3Si_3$	222.46	Organosilicon
4.	2.2677	Ethanamine, 2-(methylthio)-	C_3H_9NS	91.18	Dialkylthioethers
5.	2.2838	1,3-Propanediol	$C_3H_8O_2$	76.09	Alcohol and polyols
6.	2.2910	Trimethylsilyl fluoride	C_3H_9FSi	92.19	Organosilicon/ organohetrosilanes
7.	2.2987	Oxalic acid, cyclobutyl ethyl ester	$C_8H_{12}O_4$	172.18	Dicarboxylic acid
8.	2.3223	1H-Pyrrole, 2,5-dihydro-	C_4H_7N	69.11	Pyrrolines/alkaloids
9.	2.3453	Disopropylamine	$C_6H_{15}N$	101.19	Dialkylamine
10.	2.3536	L-Proline, 1-methyl-, methyl ester	$C_7H_{13}NO_2$	143.18	Aminoacid
11.	2.4173	Semioxamazide	$C_2H_5N_3O_2$	103.08	Aminoacid
12.	2.4280	O-ethylhydroxylamine	C_2H_7NO	61.08	Organooygen compound
13.	2.4989	2,2'-Bioxirane	$C_4H_6O_2$	86.09	Epoxides
14.	2.5508	2-Propanone, 1,1-dimethoxy-	$C_5H_{10}O_3$	118.13	Organooxygen compound/ketones
15.	2.6658	2(5H)-Furanone	$C_4H_4O_2$	84.07	Furanones
16.	2.6802	5-Isopropyl-2,4-imidazolidinedione	$C_6H_{10}N_2O_2$	142.16	Phenols
17.	2.7347	Cyclotrisiloxane, hexamethyl-	$C_6H_{18}O_3Si_3$	222.46	Organosilicon
18.	2.7501	6-Methyl-1,5 diazabicyclohexane	$C_5H_{10}N_2$	98.15	Diazinanes
19.	2.7861	N-vinylimidazole	$C_5H_6N_2$	93.11	Phenolic compound
20.	2.8188	Ethyl formate	$C_3H_6O_2$	74.08	Carboxylic acid derivatives
21.	2.8257	Furfural	$C_5H_4O_2$	96.08	Aldehydes

22.	2.8469	1,3-Dioxolane, 2-ethenyl-2-methyl-	$C_6H_{10}O_2$	114.14	Ethers
23.	2.9027	1-Butanamine, N-nitro-	$C_4H_{10}N_2O_2$	118.13	Nitramines
24.	3.0000	4-Hexen-2-one	$C_6H_{10}O$	98.14	Ketones
25.	3.0820	Furan	C_4H_4O	68.07	Heteroaromatic compounds
26.	3.1281	2-Pyrrolidinone, 5-(cyclohexylmethyl)-	$C_{11}H_{19}NO$	181.27	Pyrrolidines/ alkaloids
27.	3.2555	Oxalic acid, cyclobutyl hexyl ester	$C_{12}H_{20}O_4$	228.28	Carboxylic acidDerivatives
28.	3.2914	1,3-Diazabicyclo[3.1.0]hexane	$C_4H_8N_2$	84.12	Diazinanes/ nitrogencontaining compound
29.	3.4632	Nitric acid, 1-methylethyl ester	$C_3H_7NO_3$	105.09	Organonitrates
30.	3.4741	2-Furanmethanol, 5-methyl-	$C_6H_8O_2$	112.13	Heteroaromatic compound
31.	3.5595	2-Furancarboxaldehyde, 5-methyl-	$C_6H_6O_2$	110.11	Aryl aldehyde
32.	3.6628	2,4-Dihydroxy-2,5-dimethyl-3(2H)-furan-3-one	$C_6H_8O_4$	144.13	Furanones
33.	3.6954	Cyclotetrasiloxane, octamethyl-	$C_8H_{24}O_4Si_4$	296.62	Organosilicon
34.	3.7926	5-ethoxy-3,4-dihydro-2H-pyrrole-2-carboxylicacid, ethyl ester	$C_9H_{15}NO_3$	185.22	Alpha aminoacid and derivatives
35.	3.8193	N-Butyl-tert-butylamine	$C_8H_{19}N$	129.24	Amines
36.	3.9308	3-Hexene-2,5-dione	$C_6H_8O_2$	112.13	Carbonyl compounds
37.	3.9553	Benzyl 2-chloroethyl sulfone	$C_9H_{11}ClO_2S$	218.7	Benzenoids
38.	4.0093	2-Methyl[1,3,4]oxadiazole	$C_3H_4N_2O$	84.08	Oxadiazoles
39.	4.1534	Benzofuran-5,6-diol-3-one, 2-benzy lidene-	$C_{15}H_{10}O_4$	254.24	Flavonoids
40.	4.2222	Cyclotrisiloxane, hexamethyl-	$C_6H_{18}O_3Si_3$	222.46	Organosilicon
41.	4.2520	Furaneol	$C_6H_8O_3$	128.13	Furanones
42.	4.2918	3-Acetyl-1H-pyrroline	C_6H_7NO	109.13	Benzene and substituted derivatives
43.	4.3599	2-Isopropyl-1,3-oxazol-2-ine	$C_6H_{11}NO$	113.16	Ketones
44.	4.3231	Cyclotrisiloxane, hexamethyl-	$C_6H1_8O_3Si_3$	222.46	Organosilicon
45.	4.7046	Maltol (2-methyl-3-hydroxypyrone)	$C_6H_6O_3$	126.11	Flavanoids
46.	4.7121	Toluene	C_7H_8	92.14	Toluene
47.	4.7769	Triethyl phosphate	$C_6H_{15}O_4P$	182.15	Phosphate esters
48.	4.8890	Ethanamine, N-ethyl-N-nitroso-	$C_4H1_0N_2O$	102.14	Organonitroso compound
49.	4.9674	4H-Pyran-4-one, 2,3-dihydro-3,5 -dihydroxy-6-methyl	$C_6H_8O_4$	144.13	Pyranones
50.	5.0031	Benzene, 1-ethenyl-4-methoxy-	$C_9H_{10}O$	134.18	Phenol/Anisoles
51.	5.1992	Azetidine, 1,1'-methylenebis[2-methyl-	$C_9H_{18}N_2$	154.25	Azetines
52.	5.2841	2-Methylbutanoic anhydride	$C1_0H_{18}O_3$	186.25	Dicarboxylic acid
53.	5.3508	Ethyl-1-propenyl ether	$C_5H_{10}O$	86.13	Carbonyl compound
54.	5.4187	Cyclotetrasiloxane, octamethyl-	$C_8H_{24}O_4Si_4$	296.62	Organosilicon
55.	5.4562	Benzofuran, 2,3-dihydro-	C_8H_8O	120.15	Coumarans/ phenols
56.	5.4913	1-Pyrrolidineethanamine	$C_6H_{14}N_2$	114.19	N-alkylpyrrolidines
57.	5.4981	1,2,4,5-Tetrazine-3,6-diamine	$C_2H_4N_6$	112.09	Aminotetrazines
58.	5.5860	Silane, diethylheptyloxytridecyloxy-	$C_{24}H_{52}O_2Si$	400.75	Alkoxysilanes
59.	5.6967	1-(5'-methylfurfuryl)pyrrolidine	$C_{10}H_{15}NO$	165.23	Amines
60.	5.7505	Silane, diethylheptyloxytridecyloxy-	$C_{24}H5_2O_2Si$	400.75	Organosilicon

61.	5.8398	2-Pyrrolidinone, 1-methyl-	C_5H_9NO	99.13	N-alkylpyrrolidines
62.	5.9039	Pyrazine, 2-ethyl-6-methyl-	$C_7H_{10}N_2$	122.17	N-containing compounds
63.	6.0570	m-Aminophenylacetylene	C_8H_7N	117.15	Anilines and substituted anilines
64.	6.1765	4-Hydroxy-2-methylacetophenone	$C_9H_{10}O_2$	150.17	Carbonyl compounds
65.	6.4596	4-Methoxybenzoic acid, 3-fluoro-phenyl ester	$C_{14}H_{11}FO_3$	246.23	Organofluorinated compound
66.	6.5952	m-Anisic hydrazide	$C_8H_{10}N_2O_2$	166.18	Benzoic acid and derivatives
67.	6.6257	Cyclopentasiloxane, decamethyl-	$C_{10}H_{30}O_5Si_5$	370.77	Organosilicon compounds
68.	6.7771	Benzaldehyde, 2,4-dihydroxy-6-methyl-	$C_8H_8O_3$	152.15	Phenolic compound
69.	7.0024	Anthracene, 9,10-dihydro-9-(1-methyl-propyl)-	$C_{18}H_{20}$	236.35	Carbonyl compounds
70.	7.0635	Benzofuran-2-carboxaldehyde	$C_9H_6O_2$	146.14	Alkaloids
71.	7.5241	2-Hydroxy-1-(1'-pyrrolidiyl)-1-buten-3-one	$C_8H_{13}NO_2$	155.19	Alkaloids
72.	7.6825	2(4H)-Benzofuranone, 5,6,7,7a-tetra-hydro-4,4,7a-trimethyl-, (R)-	$C_{11}H_{16}O_2$	180.24	Alkaloids
73.	7.8993	Methanesulfinyl fluoride, trifluoro-	CF_4OS	136.07	Organofluorinated compounds
74.	7.9184	Pyrrole, 2-methyl-5-phenyl-	$C_{11}H_{11}N$	157.21	Alkaloids
75.	8.1053	Quinoline, 2-ethyl-	$C_{11}H_{11}N$	157.21	Alkaloids
76.	8.2379	Benzophenone	$C_{13}H_{10}O$	182.22	Carbonyl compound
77.	8.3310	3-Buten-2-one, 4-(4-methoxyphenyl)-	$C_{11}H_{12}O_2$	176.21	Benzene and substituted derivatives
78.	8.3509	2-Methylbutanoic anhydride	$C_{10}H_{18}O_3$	186.25	Dicarboxylic acid and derivatives
79.	8.4548	2-Propenoic acid, 3-(4-methoxy-phenyl)-,methyl ester	$C_{11}H_{12}O_3$	192.21	Benzodioxoles
80.	8.5360	2-Fluorobenzoic acid, 4-nitrophenyl Ester	$C_{13}H_8FNO_4$	261.21	Depsides and depsidones
81.	8.8284	Coniferyl alcohol	$C_{10}H_{12}O_3$	180.2	Phenolic compound
82.	8.8472	Tetradecanoic acid (Myristic acid)	$C_{14}H_{28}O_2$	228.37	Fatty acid
83.	8.9880	Acetic acid, (aminooxy)-	$C_2H_5NO_3$	91.07	Carboxylic acid
84.	9.0388	6-Hydroxy-4,4,7a-trimethyl-5,6,7,7 atetrahydrobenzofuran- 2(4H)-one	$C_{11}H_{16}O_3$	196.24	Alkaloids
85.	9.7256	Hexadecanoic acid, methyl ester	$C_{17}H_{34}O_2$	270.45	Lipids/fatty acids
86.	9.9211	n-Hexadecanoic acid	$C_{16}H_{32}O_2$	256.42	Saturated fatty acid
87.	9.9633	Dibutyl phthalate	$C_{16}H_{22}O_4$	278.34	Benzenoid (plasticizer)
88.	10.0584	Cyclopentane, 1,1,3- trimethyl-	C_8H_{16}	112.21	Solvent (aliphatic, saturated)
89.	10.2950	1H-1,2,4-Triazole, 1-vinyl-	$C_4H_5N_3$	95.1	Heterocycles/ triazoles
90.	10.6019	9,12,15-Octadecatrienoic acid, methyl ester, (Z,Z,Z)-	$C_{19}H_{32}O_2$	292.46	Lipids/fatty acids
91.	10.6510	Phytol	$C_{20}H_{40}O$	296.53	Terpenoid
92.	10.7934	Cis-3-Butyl-4-vinyl-cyclopentene	$C_{11}H_{18}$	150.26	Olefins
93.	10.8581	Octadecanoic acid	$C_{18}H_{36}O_2$	284.5	Fatty acid

3.3 CT exhibited potent cytotoxicity

The anticancer potential of CT methanol extract was assessed against GBM cells (LN229) using a dose-dependent viability assay with various concentrations (0.5, 1, 5, 10, and 15 µg/ml) *via* the trypan blue exclusion method. The IC_{50} value was derived from the dose-response curve of cell growth inhibition, revealing that CT exhibited a lower half-maximal inhibitory concentration (IC_{50}) compared to the standard chemotherapeutic drug TMZ (Figure 3). The IC_{50} for CT was calculated as 1.47 µg/ml, whereas TMZ exhibited 17.24 µg/ml, indicating that CT is a more potent inhibitor of GBM cell growth than TMZ (Figure 3).

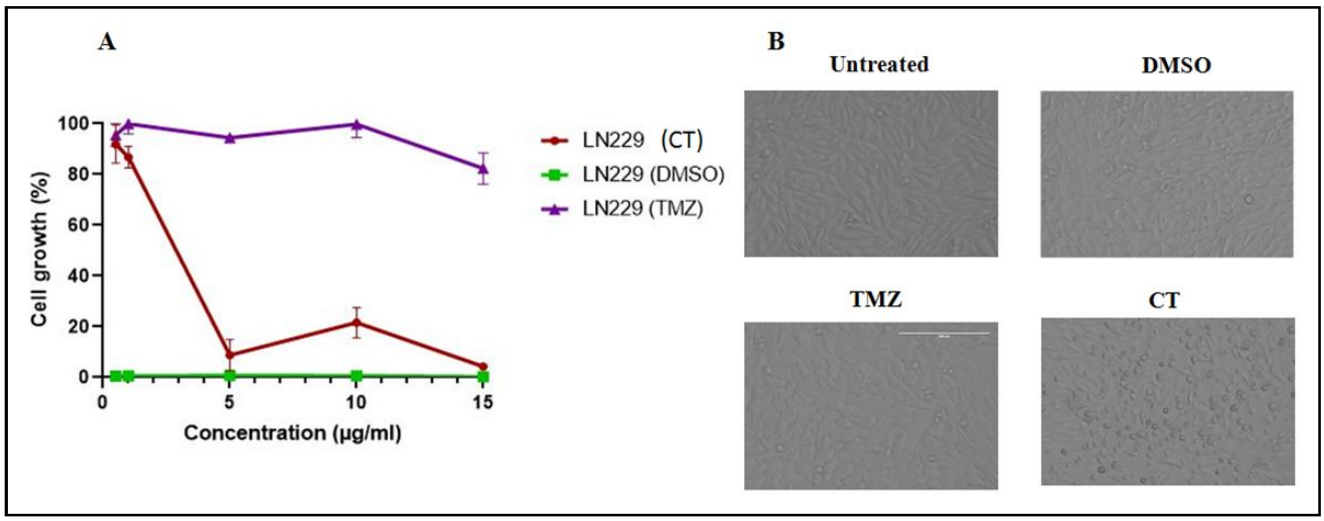

Figure 3: **Dose-dependent cytotoxicity effect of CT. The crude methanolic extract of CT exhibited a concentration-dependent cytotoxic effect on LN229 cells. The cytotoxicity effects of (A) CT leaf extract, TMZ, and DMSO and (B) the representative images of control (untreated), CT treated, DMSO, and TMZ in LN229 cells were captured using phase contrast microscopy. The mean ± standard error values were reported with biological and technical replicates (n=4), with $p<0.05$ for CT vs. DMSO (one-way ANOVA).**

3.4 CT arrests cells at the G1/S phase

Fluorescence-based ubiquitination cell cycle analysis was performed to investigate the impact of CT on cell cycle progression. The analysis utilizes two proteins, Cdt1 (linked to red fluorescent protein) and geminin (linked to green fluorescent protein), which bind to specific phases of the cell cycle. Following CT treatment, a reduction in Cdt1 levels led to an increased visibility of red fluorescent nuclei, indicating cell cycle arrest at the G1/S transition. This result was further confirmed through fluorescent microscopy, demonstrating that CT induces cell cycle arrest in the G1/S phase (Figure 4).

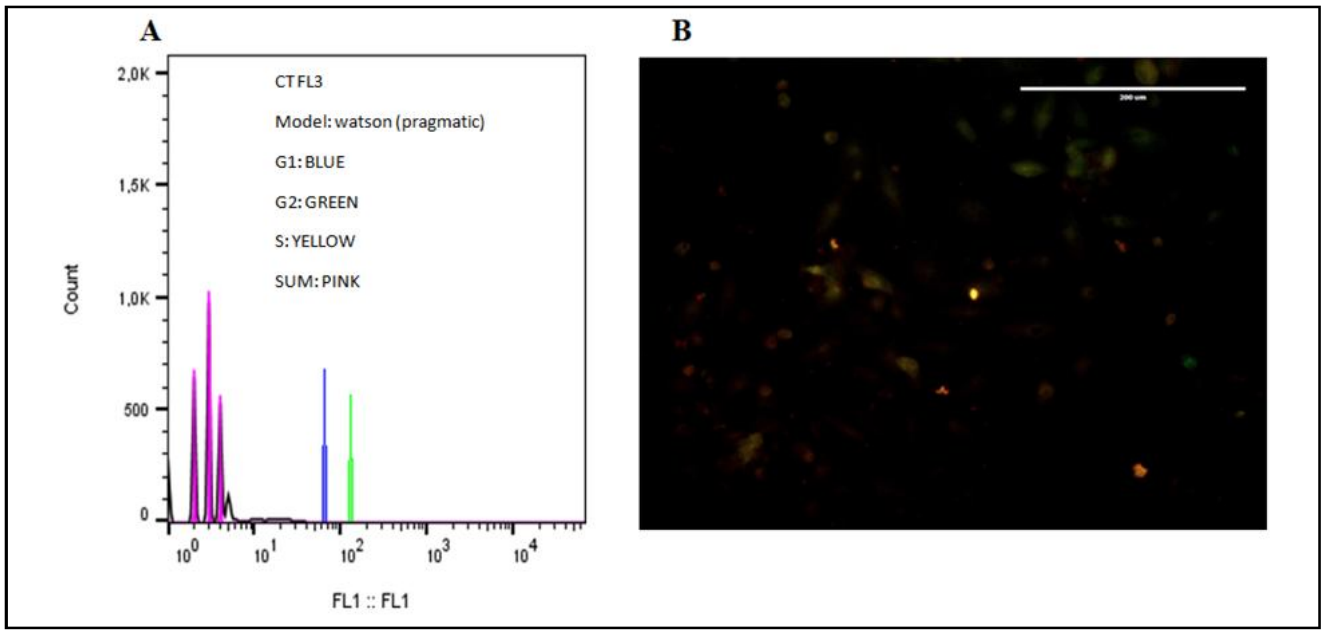

Figure 4: **Cell cycle analysis of CT. The cell-cycle analysis of CT was conducted by using the FUCCI biosensor in a flow cytometer (A) showed arrest at the G1/S phase and (B) the representative image demonstrating the impact of CT on LN229 cells exhibited red, green, and yellow fluorescence indicating cell cycle arrest.**

3.5 Drug likeness and pharmacokinetic properties of CT

An *in silico* analysis was performed to assess the drug-likeness and pharmacokinetic profile of the identified compounds including their ADMET properties such as absorption, distribution, metabolism, excretion, and toxicity. Out of the 93 identified compounds, 54 exhibited drug-like characteristics with a molecular weight below 300 Da, meeting all criteria of the "Lipinski rule of five" and indicating potential for biological activity. Gastrointestinal permeation was notably effective in 56 metabolites, suggesting good absorption characteristics.

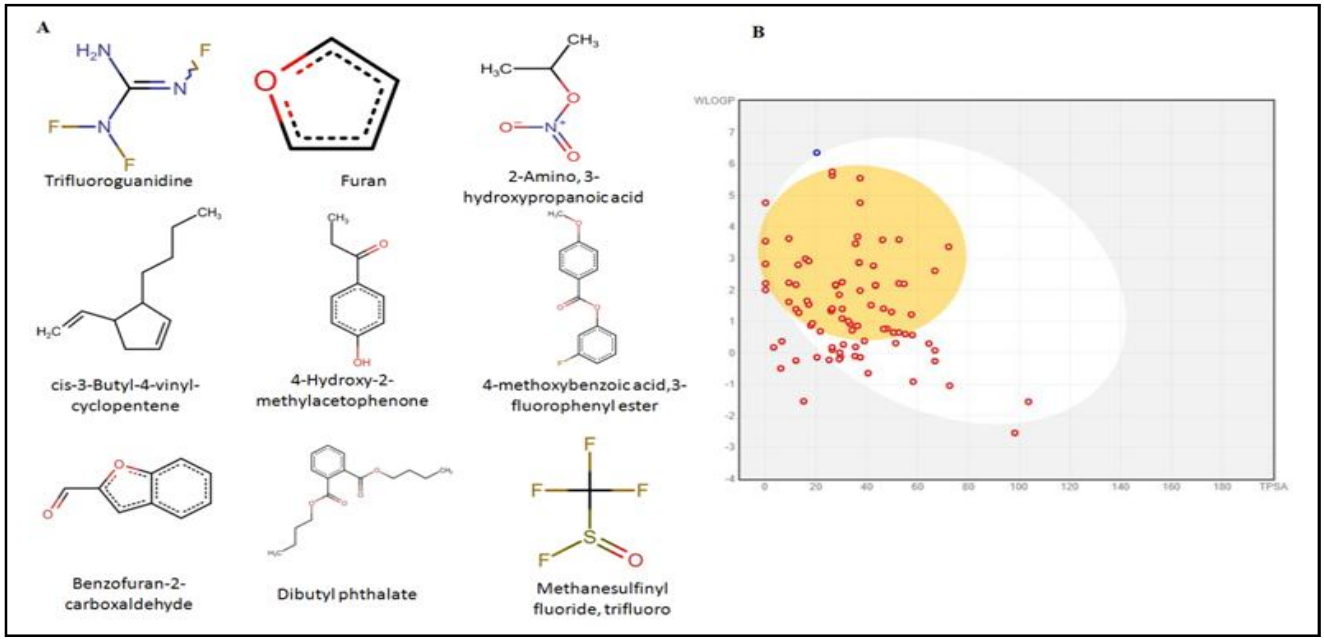

Figure 5: The compounds of CT with drug-likeness property (A) shows the configurations of compounds devoid of any toxicity that were depicted using the swissADME online software tool (B) the model of a boiled egg, symbolizing compounds with BBB permeability in the yellow region and GI permeability in the white region, was illustrated.

Table 2: *In silico* analysis for predicting the pharmacokinetic and drug likeness properties of the top lead drug candidates of CT. GI-gastrointestinal absorption, BBB-Blood brain barrier permeability, P-gp- P-glycoprotein, CYP-cytochrome P450, AMES-mutagenicity, renal OCT2-renal organic cation transporter 2.

Parameters		Trifluoro guanidine	2-amino, 3-hydroxy propanoic acid	Furan	Cis-3-Butyl-4-vinyl -cyclo pentene	4-Hydroxy-2-methyl aceto phenone phenyl ester	4 methoxy benzoic acid, 3-fluoro	Benzo furan-2-carbox aldehyde	Methane sulfinyl fluoride, trifluoro	Dibutyl phthalate
Absorption	Water solubility	Very soluble	Very soluble	Very soluble	Soluble	Soluble	Soluble	Soluble	Very Soluble	Soluble
	GI absorption	High	High	High	High	High	High	High	High	High
Distribution	BBB permeability	Yes	Yes	Yes	Yes	Yes	Yes	Yes	Yes	Yes
	Pgp substrate	No	No	No	No	No	No	No	No	No
Metabolism	CYP1A2 inhibitor	No	No	No	No	Yes	Yes	Yes	No	Yes
	CYP2C19 inhibitor	No	No	No	No	No	Yes	No	No	Yes
	CYP2C9 inhibitor	No	No	No	Yes	No	No	No	No	No
	CYP3A4 inhibitor	No	No	No	No	No	No	No	No	No
Excretion	Renal OCT2 substrate	No	No	No	No	No	No	No	No	No
	Hepatotoxicity	No	No	No	No	No	No	No	No	No
	AMES	No	No	No	No	No	No	No	No	No
	Skin sensitization	No	No	No	No	No	No	No	No	No
Drug likeness	Lipinski violations	0	0	0	0	0	0	0	0	0

A total of 59 identified compounds exhibited the capability to cross the BBB, highlighting their potential efficacy in central nervous system applications. P-glycoprotein inhibition, which can increase drug bioavailability, was observed in several lead compounds. Furthermore, the study identified compounds that act as inhibitors of Cytochrome P450 enzymes (CYP1A2, CYP2C19, CYP2D6, and CYP3A4), which play a crucial role in drug metabolism.

Toxicity predictions indicated that 9 compounds were non-mutagenic, non-hepatotoxic, and non-inducers of skin sensitization. The 9 compounds, comprising alkaloids, organoelements, and organic compounds, exhibit promising drug-like properties with minimal toxic effects (Figure 5, Table 2).

4. Discussion

The development of new anticancer medications remains a daunting challenge due to the adverse effects of newly developed drugs and the increasing incidence of multi-drug resistance. Natural polyphenols, however, offer significant promise for cancer therapy, including glioblastoma multiforme, owing to their therapeutic potential and relatively low side effects. In this study, the crude methanol leaf extract of *C. tagal* was assessed for its polyphenolic content using high-performance thin-layer chromatography. This analysis confirmed the presence of flavonoids, phenols, saponins, and alkaloids, with distinct bands observed at UV 254 and 366 nm, indicating their substantial role in the extract's bioactivity.

The cytotoxic potential of *C. tagal* was further supported by gas chromatography-mass spectrometry, which identified 93 metabolites in the methanol extract. These metabolites, including polyphenols, saponins, and alkaloids, are known to exhibit anticancer, antioxidant, and anti-inflammatory properties, which likely contributed to the observed cytotoxicity in LN229 GBM cells (Rajesh, 2020; Kumari *et al*., 2021; Weber *et al*., 2008; Vasanthakumar *et al*., 2024). Notably, compounds such as n-hexadecanoic acid, 2(5H)-furanone, azetidine, 1,2,4-triazole, and quinoline have demonstrated broad-spectrum activities, including anti-inflammatory, antiviral, antifungal, and antioxidant effects (Patel and Singh, 2023). It is clearly evident that the *C. tagal* was more effective with less IC_{50} than the current GBM drug, temozolomide. These results are consistent with earlier studies demonstrating the potent cytotoxic effects of polyphenols on different cancer cell lines, further supporting the therapeutic potential of *C. tagal* as an anti-GBM agent (Bakrim *et al*., 2022).

The fluorescence ubiquitination cell cycle (FUCCI) sensor revealed that *C. tagal* effectively arrests the progression of GBM cells at the G1/S phase. This suggests that the polyphenols in the extract may exert their therapeutic effect during this phase of the cell cycle.

The failure of drugs during clinical trials often results from toxicity and poses substantial financial challenges. In this context, pre-clinical validation through *in silico* analysis becomes indispensable for assessing the efficacy and safety profiles of drug candidates. ADMET properties are critical factors in drug development and often contribute to the failure of numerous drugs during clinical trials (Zhong *et al*., 2017). Poor solubility, limited gastrointestinal absorption, and the inability to cross the blood-brain barrier (BBB) are key factors that hinder the development of effective drugs. In this study, 93 compounds from *C. tagal* were evaluated for their pharmacokinetic characteristics and drug-likeness. Out of these, 54 compounds were found to have the ability to penetrate the BBB, while 56 compounds exhibited high gastrointestinal absorption. Additionally, 49 compounds demonstrated significant water solubility, indicating their potential as bioavailable drug candidates.

Toxicity profiling revealed 9 compounds that were non-mutagenic, non-hepatotoxic, and non-sensitizing to the skin, laying the groundwork for further investigation into their therapeutic potential. These findings are particularly important for the identification of safe and effective lead compounds for drug development. The lead compounds include trifluoro guanidine, 2-amino, 3-hydroxypropanoic acid, Furan, Cis-3-Butyl-4-vinyl-cyclopentene, 4-Hydroxy-2-methylacetophenone, 4 methoxy benzoic acid,3-fluorophenyl ester, benzofuran-2-carboxaldehyde, methane sulfinyl fluoride, trifluoro, dibutyl phthalate. Among the 9 primary drug-like candidates identified based on ADMET characteristics, several compounds, including trifluoroguanidine, furan, and 4-hydroxy-2-methylacetophenone, demonstrated promising bioavailability and bioactivity. Trifluoroguanidine, an alkaloid, has been shown to possess analgesic, anticancer, antihypertensive, and antipyretic properties, further supporting the therapeutic value of these compounds(Bakrim *et al.*, 2022; Ng *et al*., 2015). These nine compounds from *C. tagal* likely contribute to its potent cytotoxic effects against GBM cells, further highlighting the superior therapeutic potential of *C. tagal* extract as a promising drug candidate, surpassing the efficacy of the chemotherapeutic agent TMZ. Given the potential lower toxicity and adverse reactions of these compounds compared to conventional chemotherapeutic agents, *C. tagal* holds promise as a safer alternative for GBM treatment. However, clinical studies are required to verify the therapeutic efficacy of these compounds in humans.

5. Conclusion

This study provides compelling evidence supporting the presence of key polyphenolic compounds, including alkaloids, saponins and flavonoids in *C. tagal* through HPTLC fingerprinting. Additionally, GC-MS analysis identified secondary metabolites responsible for various biological activities, including significant antioxidant properties. Computational predictions further suggest that these metabolites, particularly polyphenols and alkaloids, exhibit promising drug-like characteristics, with lower toxicity profiles compared to conventional synthetic compounds. The findings underscore *C. tagal* as a potent candidate for glioblastoma treatment. However, further validation through rigorous *in vitro* studies is necessary to ascertain its therapeutic potential and establish its viability as a clinical drug for glioblastoma therapy.

Acknowledgments

The authors express their gratitude to Lady Doak College, Madurai for instrumental support. MM acknowledges the Tampere University for granting access to the instrumentation facility to conduct *in vitro* cytotoxicity assays with GBM cells. We acknowledge the funding agency, DST-FIST for HPTL Instrumentation support

Conflict of interest

The authors declare no conflicts of interest relevant to this article.

References

Abideen, Z.; Qasim, M.; Rasheed, A.; Yousuf Adnan, M.; Gul, B and Ajmal Khan, M. (2015). Antioxidant activity and polyphenolic content of phragmites karka under saline conditions. Pakistan Journal of Botany, **47**(3):813-818.

Arivuselvan, N.; Silambarasan, D.; Govindan, T. and Kathiresan, K. (2011). Antibacterial activity of mangrove leaf and bark extracts against human pathogens. Advances in Biological Research, **5**(5):251-254.

Bakrim, S.; El Omari, N.; El Hachlafi, N.; Bakri, Y.; Lee, L. H. and Bouyahya, A. (2022). Dietary phenolic compounds as anticancer natural drugs: recent update on molecular mechanisms and clinical trials. Foods, **11**(21):1-33.

Boopathy, N. S.; Kandasamy, K.; Subramanian, M. and You-Jin, J. (2011). Effect of mangrove tea extract from *Ceriops decandra* (Griff.) Ding Hou. on salivary bacterial flora of DMBA Induced Hamster Buccal Pouch carcinoma. Indian Journal of Microbiology, **51**(3):338-344.

Chacha, M. (2012). Comparative anticancer activity of dolaborane diterpenes from the roots of *Ceriops tagal* (Rhizophoraceae). International Journal of Biological and Chemical Sciences, **6**(2): 913-919.

Shu-Jun Ni; Jun Li. and Min-Yi Li (2018). Two new dolabranes from the Chinese mangrove *Ceriops tagal*. Chemistry and Biodiversity, **15**(3): e1700563.

Costa, M.; Sezgin-Bayindir, Z.; Losada-Barreiro, S.; Paiva-Martins, F.; Saso, L. and Bravo-Díaz, C. (2021). Polyphenols as antioxidants for extending food shelf-life and in the prevention of health diseases: Encapsulation and interfacial phenomena. Biomedicines, **9**(12):1909.

Cragg, G. M. and Newman, D. J. (2005). Plants as a source of anticancer agents. Journal of Ethnopharmacology, **100**(1-2):72-79.

Daina, A.; Michielin, O. and Zoete, V. (2017). SwissADME: A free web tool to evaluate pharmacokinetics, drug-likeness and medicinal chemistry friendliness of small molecules. Scientific Reports, pp:7:42717.

Doan, P.; Musa, A.; Murugesan, A.; Sipilä, V.; Candeias, N. R.; Emmert-Streib, F.; Ruusuvuori, P.; Granberg, K.; Yli-Harja, O. and Kandhavelu, M. (2020). Glioblastoma multiforme stem cell cycle arrest by alkylamino-phenol through the modulation of EGFR and CSC signaling pathways. Cells, **9**(3), 681.

Eswaraiah, G.; Peele, K. A.; Krupanidhi, S.; Indira, M.; Kumar, R. B. and Venkateswarulu, T. C. (2020). GC-MS analysis for compound identification in leaf extract of *Lumnitzera racemosa* and evaluation of its *in vitro* anticancer effect against MCF7 and HeLa cell lines. Journal of King Saud University-Science, **32**(1):780-783.

Fisher, J. P. and Adamson, D. C. (2021). Current FDA-approved therapies for high-grade malignant gliomas. Biomedicines, **9**(3):324.

Ferlay J; Ervik M.; Lam F.; Laversanne M.; Colombet M.; Mery L.; Piñeros M.; Znaor A.; Soerjomataram I. and Bray F. (2024). GLOBOCAN report, 2022, CA Cancer J. Clin., **74**(3):229-263.

Jain, K. K. (2018). A critical overview of targeted therapies for glioblastoma. Frontiers in Oncology, 8:419.

Kandler, H.; Bleisch, M.; Widmer, V. and Reich, E. (2009). A validated HPTLC method for the determination of illegal dyes in spices and spice mixtures. Journal of Liquid Chromatography and Related Technologies, **32**(9):1273-1288.

Kiran Kumar, M. and Pola, S. (2022). Mangrove species as a potential source of bioactive compounds for diverse therapeutic applications. Marine Antioxidants: Preparations, Syntheses, and Applications, pp: 249-263.

Krex, D.; Klink, B.; Hartmann, C.; Von Deimling, A.; Pietsch, T.; Simon, M.; Sabel, M.; Steinbach, J. P.; Heese, O.; Reifenberger, G.; Weller, M. and Schackert, G. (2007). Long-term survival with glioblastoma multiforme. Brain, **130**(10):2596-2606.

Kumari, M.; Tahlan, S.; Narasimhan, B.; Ramasamy, K.; Lim, S. M.; Shah, S. A. A.; Mani, V. and Kakkar, S. (2021). Synthesis and biological evaluation of heterocyclic 1,2,4-triazole scaffolds as promising pharmacological agents. BMC Chemistry, **15**(5):1-16.

Makkar, R.; Behl, T.; Bungau, S.; Zengin, G.; Mehta, V.; Kumar, A.; Uddin, M. S.; Ashraf, G. M.; Abdel-Daim, M. M.; Arora, S. and Oancea, R. (2020). Nutraceuticals in neurological disorders. International Journal of Molecular Sciences, **21**(12):1-19.

Manohar, S. M.; Yadav, U. M.; Kulkarnii, C. P. and Patil, R. C. (2023). An overview of the phytochemical and pharmacological profile of the spurred mangrove *Ceriops tagal* (Perr.) C. B. Rob. Journal of Natural Remedies, **23**(1):57-72.

Murugesan, M.; Theivendram, T.; Thangapandian, R. and Murugesan, A. (2020). Survey of the ethnomedicinal use of marine halophytes among the indigenes of coastal regions of Tamil Nadu, India. Phytocoenologia, **50**(2):173-186.

A. Narmadha Devi; K. Sundharaiya; J. Rajangam,; M. Gnanasekaran; A. Vijayasamundeeswari and M. Kabilan (2024). Biochemical and phytochemical analysis of yardlong bean (*Vigna unguiculata* (L.) Verdc. subsp. sesquipedalis) using gas chromatography and mass spectroscopy (GC-MS). Ann. Phytomed., 13(2):812-821.

Ng, Y. P.; Or, T. C. T., and Ip, N. Y. (2015). Plant alkaloids as drug leads for alzheimer's disease. Neurochemistry International, **89**:260-270.

Pandey, M. M.; Rastogi, S. and Rawat, A. K. S. (2013). Indian traditional ayurvedic system of medicine and nutritional supplementation. Evidence-Based Complementary and Alternative Medicine, **2013**(01):1-12.

Ranjith Kumar, S.; Chozhan, K.; Murugesh, K. A.; Rajeswari, R. and Kumaran, K. (2021). Gas chromatography-mass spectrometry analysis of bioactive compounds in chloroform extract of *Psoralea corylifolia* L. Journal of Applied and Natural Science, **13**(4):1225-1230.

Sakaue-Sawano, A., Kurokawa, H., Morimura, T., Hanyu, A., Hama, H., Osawa, H. and Miyawaki, A. (2008). Visualizing spatiotemporal dynamics of multicellular cell-cycle progression. Cell, **132**(3):487-498.

Sun, W.; Kalen, A. L.; Smith, B. J.; Cullen, J. J. and Oberley, L. W. (2009). Enhancing the antitumor activity of adriamycin and ionizing radiation. Cancer Research, **69**(10):4294-4300.

Tiwari, P.; Tamrakar, A. K.; Ahmad, R.; Srivastava, M. N.; Kumar, R.; Lakshmi, V. and Srivastava, A. K. (2008). Antihyperglycaemic activity of *Ceriops tagal* in normoglycaemic and streptozotocin-induced diabetic rats. Medicinal Chemistry Research, **17**(2):74-84).

Tundis, R.; Menichini, F. and Loizzo, M. R. (2014). Recent insights into the emerging role of triterpenoids in cancer therapy: Part II. Studies in Natural products Chemistry, **41**:1-32.

Vasanthkumar, S.S.; Prabha, T.; Shenbagavalli, S.; Rajangam, J.; Vallal Kannan, S. and Baskaran, A. (2024). Exploring the therapeutic potential of bioactive compounds in spices and herbs: Preclinical evidence and medicinal applications. Ann. Phytomed, **13**(2):230-237.

Weber, B.; Herrmann, M.; Hartmann, B.; Joppe, H.; Schmidt, C. O. and Bertram, H. J. (2008). HPLC/MS and HPLC/NMR as hyphenated techniques for accelerated characterization of the main constituents in chamomile (*Chamomilla recutita* [L.] Rauschert). European Food Research and Technology, **226**(4):755-760.

Williams, R. J.; Spencer, J. P. E. and Rice-Evans, C. (2004). Flavonoids: Antioxidants or signalling molecules? Free Radical Biology and Medicine, **36**(7):838-849.

Wu, Y. C.; Cao, L.; Mei, W. J.; Wu, H. Q.; Luo, S. H.; Zhan, H. Y. and Wang, Z. Y. (2018). Bis-2(5H)-furanone derivatives as new anticancer agents: Design, synthesis, biological evaluation, and mechanism studies. Chemical Biology and Drug Design, **92**(1):1232-1240.

Yamajala B.R.D. Rajesh. (2020). Quinoline heterocycles: Synthesis and bioactivity, pp:1-18.

Zhang, Y.; Deng, Z.; Gao, T.; Proksch, P. and Lin, W. (2005). Tagalsins A-H, dolabrane-type diterpenes from the mangrove plant, *Ceriops tagal*. Phytochemistry, **66**(12):1465-1471.

Zhong, H. A. (2017). ADMET properties: Overview and current topics. Drug design: Principles and Applications. pp:113-133.

Citation **Monica Murugesan, Sankar Natesan and Priyatharsini Rajendran (2025). Pharmacological evaluation and cytotoxic assessment of *Ceriops tagal* (Perr.) C.B. Rob. metabolites with comprehensive analytical and ADMET insights against Glioblastoma Multiforme. Ann. Phytomed., 14(1):569-579. http://dx.doi.org/10.54085/ap.2025.14.1.54.**